Advanced Diagnostic Technique for Alzheimer's Disease using MRI Top-Ranked Volume and Surface-based Features

Esraa M. Arabi[1], Khaled S. Ahmed[2]*, Ashraf S. Mohra[2]

[1]MSc, Department of Electrical Engineering, Benha Faculty of Engineering, Benha University, Benha, Egypt
[2]PhD, Department of Electrical Engineering, Benha Faculty of Engineering, Benha University, Benha, Egypt

ABSTRACT

Background: Alzheimer's disease (AD) is the most dominant type of dementia that has not been treated completely yet. Few Alzheimer's patients are correctly diagnosed on time. Therefore, diagnostic tools are needed for better and more efficient diagnoses.

Objective: This study aimed to develop an efficient automated method to differentiate Alzheimer's patients from normal elderly and present the essential features with accurate Alzheimer's diagnosis.

Material and Methods: In this analytical study, 154 Magnetic Resonance Imaging (MRI) scans were obtained from the Alzheimer's Disease Neuroimaging Initiative (ADNI) database, preprocessed, and normalized by the head size for extracting features (volume, cortical thickness, Sulci depth, and Gyrification Index Features (GIF). Relief-F algorithm, t-test, and one way-ANOVA were used for feature ranking to obtain the most effective features representing the AD for the classification process. Finally, in the classification step, four classifiers were used with 10folds cross-validation as follows: Gaussian Support Vector Machine (GSVM), Linear Support Vector Machine (LSVM), Weighted K-Nearest Neighbors (W-KNN), and Decision Tree algorithm.

Results: The LSVM classifier and W-KNN produce a testing accuracy of 100% with only seven features. Additionally, GSVM and decision tree produce a testing accuracy of 97.83 % and 93.48 %, respectively.

Conclusion: The proposed system represents an automatic and highly accurate AD detection with a few reliable and effective features and minimum time.

Keywords

Hippocampus; Amygdala; Cortical Thickness; Gyrification Index; Sulcal Depth; Alzheimer Disease; Relief Algorithm

Introduction

Alzheimer's disease (AD) is a progressive neurodegenerative disease without any certain treatment until now and leads to death eventually. In addition, AD mainly affects older people over the age of 65 years with an exponentially increasing rate, nearly doubling every five years [1]. However, Alzheimer's has no definitive cure [2,3], and the detection of the disease in the early stage can enormously assist in slowing down the progress, leading to effective treatment.

Some tests are used to diagnose Alzheimer's, such as mini-mental exams [4], distinguishing the cognitive symptoms of the disease, and

*Corresponding author: Khaled S. Ahmed
Department of Electrical Engineering, Benha Faculty of Engineering, Benha University, Benha, Egypt
E-mail: khaled.sayed@bhit.bu.edu.eg

Received: 3 December 2021
Accepted: 20 March 2022

brain imaging techniques, such as Magnetic Resonance Imaging (MRI) [5-8]. The neuropathological alteration due to AD can appear much earlier before the onset of clinical symptoms [9]. Therefore, the early detection of AD using neuroimaging techniques is considered a promising area of research, especially with the advances in machine-learning and image-segmentation techniques [10-16].

MRI scans have been investigated to obtain many Alzheimer's biomarkers and study the most atrophic regions using volume measurements [6,17], shape [18], texture [17,19,20], cortical measurements [21,22], and sulcal measurements [23]. These measurements were applied to many brain regions, such as the hippocampus [24], which is one of the earliest brain regions in the neurodegeneration [25], amygdala [26,27], whole brain [28], entorhinal cortex [29], brainstem [30], and ventricles [31]. Recent advances in machine-learning techniques, such as Support Vector Machine (SVM) [32,33], Naïve Bayes, Logistic Regression, and K-Nearest Neighbors (KNN) [34] have been implemented. The use of automated methods rather than relying solely on physician experiments has led to the reliance on ensemble models to improve disease detection and increase accuracy. However, a major challenge is in selecting the best biomarkers that characterize AD to differentiate between AD and Normal Controls (NC).

Several feature selection methods have been used in recent studies; for example, Particle Swarm Optimization (PSO) algorithm [35], genetic algorithm, t-test [36,37], and Principal Component Analysis (PCA) [38-41].

The current study aimed to demonstrate the least and most beneficial number of features among a large pool of different AD biomarkers to classify AD cases and perform the best classifiers using these features.

Material and Methods

Database

In this analytical study, data were acquired from the Alzheimer's disease Neuroimaging Initiative (ADNI) database (http://adni.loni.usc.edu), propelled as a public-private corporation by six nonprofit organizations in 2003 as follows: the National Institute on Aging (NIA), the National Institute of Biomedical Imaging and Bioengineering (NIBIB), the Food and Drug Administration (FDA), and private pharmaceutical companies. ADNI's main objective was to check whether some specific biomarkers, clinical and neuropsychological assessment, positron emission tomography (PET), and serial MRI can be combined to evaluate the Mild Cognitive Impairment (MCI) evolution and early Alzheimer's.

154 T1-weighted images were obtained from ADNI, 37 female cases and 41 male cases in the AD stage, and 40 females and 36 males in the normal control (NC) stage. The age ranged from 50 to 85 years. The magnetic field strength was 3T, slice thickness was 1.2 mm, acquisition matrix was 240 ×256 pixels with pixel spacing X=1.0 mm; pixel spacing Y=1.0 mm, the number of slices = 176, and demographic characteristics of the individuals (shown in Table 1).

Image Preprocessing

Before executing the analysis, the quality of the data must be improved due to missing values and inaccurate information, leading to

Table 1: Sample size for classes

Class	Female	Male	Sample size/each class
Alzheimer's Disease Patients (AD)	37	41	78
Normal Control (NC)	40	36	76

distorted results. The data was preprocessed using CAT12 after obtaining it from ADNI. The preprocessing workflow involved bias field inhomogeneities correction, affine registration, skull stripping, and normalization to Montreal Neurological Institute (MNI). Hammers atlas [42] is then used as a binary mask to select the brain Regions of Interest (ROIs), as shown in Figure 1. Finally, 71 raw volumetric measurements, 68 cortical thickness (CT), 68 gyrification indexes (GI), and 68 sulcal depth (SD) measurements are extracted. The four measurements, together with their differences among AD and NC, are shown in Figure 2. Volume measurements, involving the hippocampus, amygdala, temporal pole, fusiform, insula, putamen, thalamus, lateral temporal ventricle, and cuneus were normalized by the intracranial volume. Relative volumes provide more precise volumes to reduce the influence of factors, such as the head and brain size.

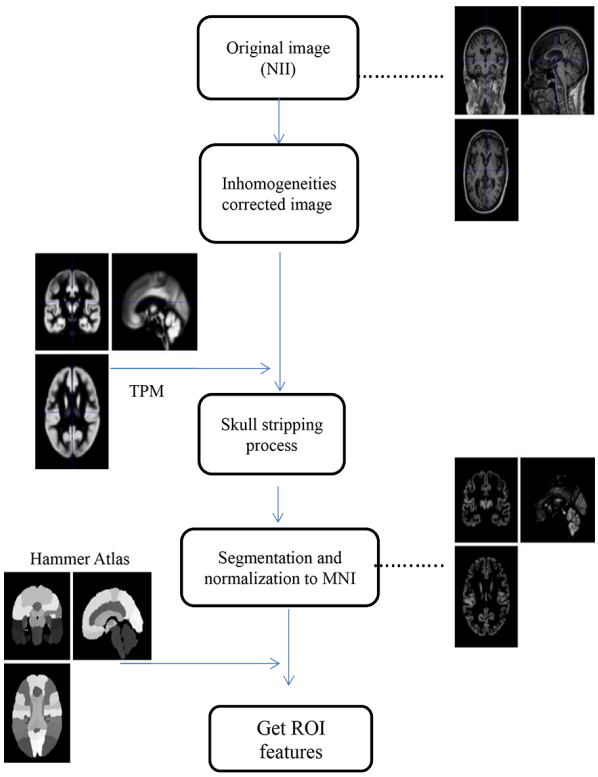

Figure 1: Workflow of medical image preprocessing

Entorhinal, temporal pole, fusiform, parahippocampus, and insula are examples of surface-based characteristics (CT, GI, and SD), resulting in the excellent features to indicate the existence of the disease.

Feature Selection

Feature selection uses specific algorithms to select the most relevant features with the most contribution towards predicting variables for increasing the accuracy and reducing the prediction time. A high-dimensional feature vector, 71 volumetric, and 68×3 surface-based features (cortical thickness, sulcal depth, and gyrification index) were in this study without any significant or appropriate information to diagnose AD. Therefore, the following algorithms are used to obtain the top-ranked features, including the Relief-F algorithm, t-test, and one-way ANOVA.

Relief-F Algorithm

Relief-F is one of the filter methods used for feature selection that is particularly sensitive to feature interactions [43], designed originally for binary classification, and replaced with Relief-F as the most utilized algorithm [44].

This algorithm aimed to assess the quality of features according to the ability of their values to separate between the cases that are close to each other [45], including three important steps: the nearest hit and miss, calculation of the weights of features, and presentation of a ranked list of features. Based on this list of features, the top 12 ranked optimal features were selected. The t-test is a statistical test to determine a difference in the means of two samples and either dependent or independent samples. T-tests were used as a feature ranking algorithm in a variety of machine-learning studies [46,47]. The formula of the t-test is defined as follows:

$$\text{t}-\text{value} = \frac{\mu_1 - \mu_2}{\sqrt{\frac{\sigma_1^{\,2}}{n_1} + \frac{\sigma_2^{\,2}}{n_2}}} \quad (1)$$

where n_1, n_2 are the number of samples, μ_1,

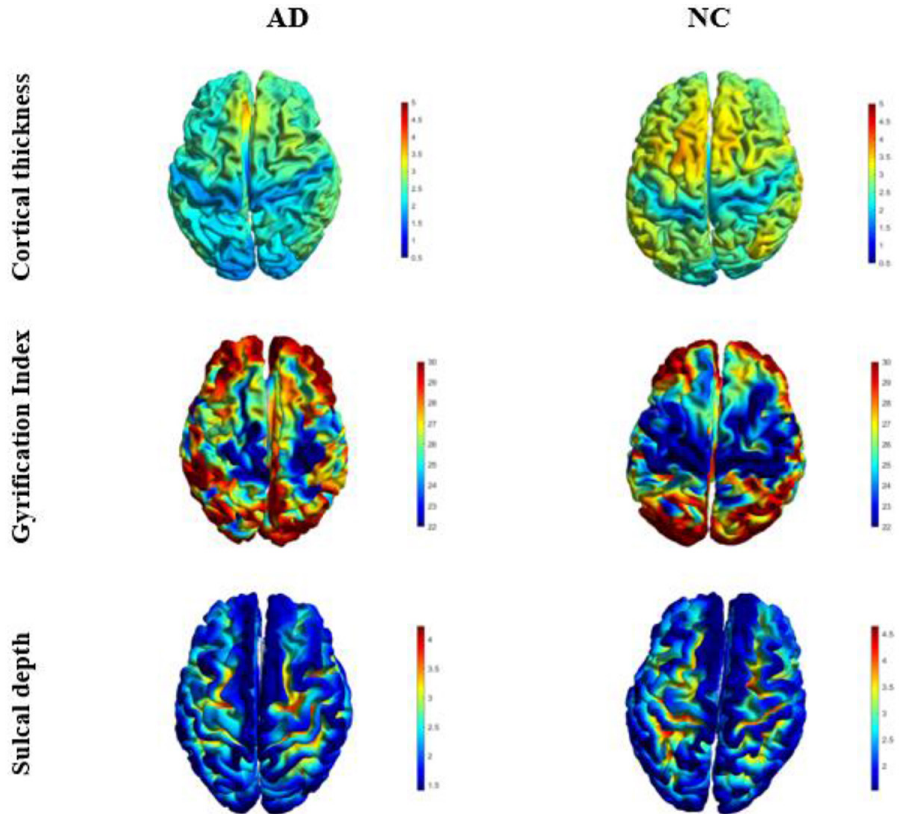

Figure 2: Brain mapping of cortical thickness, gyrification index, and sulcus depth maps estimated using CAT12 toolbox. Each column denotes a subject in the normal control (NC) and Alzheimer's disease (AD) groups.

μ_2 are the means, and σ_1, σ_2 are the standard deviation of two classes.

T-value measures the significance of the difference between two samples relative to the variation in each sample. Therefore, the high t-value of a specific feature for the two samples AD and NC leads to reliability in the classification and selection.

The absolute t-value for each feature was computed, and all features were ranked depending on their t-values. The 12 top discriminative features were selected.

One Way ANOVA

ANOVA stands for analysis of variance was used to compare the sample means for two independent groups, or more, determining whether one group has a statistically significant difference in its mean than the others based on the following formula:

$$\text{F}-\text{value}=\frac{MS_b}{MS_w} \tag{2}$$

$$\text{MS}_\text{b}=\frac{\sum_{\text{i=1}}^{\text{k}}\text{n}_\text{i}\left(\overline{\text{x}_\text{i}}-\overline{\text{x}}\right)^2}{\text{k}-1} \tag{3}$$

$$\text{MS}_\text{w}=\frac{\sum_{\text{i=1}}^{\text{k}}\sum_{\text{j=1}}^{\text{n}}\left(\text{x}_\text{ij}-\overline{\text{x}}_\text{i}\right)}{\text{n}-\text{k}} \tag{4}$$

where F is the variance ratio for the overall test, MS_b is the mean square between groups, MS_w is the mean square within groups, k is the number of classes, and n is the number of observations.

The F-value was measured for all features and ranked from the highest F-value to the lowest; the 12 top-ranked features were then

obtained.

Classification

Support Vector Machine (SVM)

SVM is a discriminative classifier for the selection of the best hyper-plane or a group of hyper-planes that maximizes the distance of the margin to classify the data into many classes. The hyperplane is defined by the following equation:

$$g(x)=wTx+b$$

where w is the weight vector, and b is the offset parameter for the input vector x.

The maximum and minimum margin widths are 2/(||w||) and 1/2 ||w||, respectively.

For non-linearly separable data, SVM uses a kernel function with an added dimension to the data and transforms data to a higher-dimensional space, such as the Gaussian kernel defined [48] as follows:

$$(x,y)=exp(-\gamma|x-y|^2)$$

where γ is gamma, and $|x-y|^2$ is defined as squared Euclidean distance between the two feature vectors. The gamma hyperparameter (γ) controls the training points, which affected the decision boundary.

K-Nearest Neighbor

In the training phase, K-Nearest Neighbor, as one of the simplest supervised machine-learning classifiers, stores and arranges all labeled data in the memory. Therefore, it is memory-based without any need to model fitting and classifies the test point based on a similarity measure between the test point and its nearest neighbors. For example, with x0 as a new point, the k-nearest neighbor search obtained the k closest points in distance to x0. Among these k neighbors, the number of the data points in each class was counted. Based on the most votes from the neighbors, the data point is classified.

Weighted KNN takes the majority votes from the neighbors without caring about their distance from the test point.

Decision Tree

The decision tree is a classification model in a shape of a diagram used in data analysis. In the training step, this algorithm aimed to divide the data into smaller sets of data based on a specific feature. The node in the tree states a condition of a feature; each branch falling from that node corresponds to one of the possible attribute values. Each leaf represents class labels related to the case. Cases in the training set are classified by guiding them from the tree's root down to a leaf, depending on the result of the tests.

Results

A total of 154 individuals participated in this study, 108 and 46 for the training and testing the performance of classifiers, respectively. The features were organized into four main groups: volume features, cortical thickness, sulcal depth, and gyrification index. Volume was measured for 71 regions of interest (ROI) in the brain. Each of the other three features was measured for 68 ROI, as explained in Appendix 1.

The t-test, Relief-F algorithm, and ANOVA were used for the feature ranking process and selected the 12 top-ranked features from each of them, as indicated in Table 2. The 9 common features were selected among the 12 top-ranked features (group1), including the right amygdala, cortical thickness left entorhinal, left amygdala, left hippocampus, cortical thickness right entorhinal, right ambient and parahippocampus, right hippocampus, left ambient and parahippocampus, and left inferior middle temporal gyri.

A total of 9 top-ranked features were then selected, and then the 7 common features were selected among the 9 features. The 7 Common features were considered group2, including the right amygdala, cortical thickness left entorhinal, left Amygdala, left hippocampus, right ambient and parahippocampus, right hippocampus, left ambient, and parahippocampus.

The four classifiers, such as decision tree, linear SVM, Gaussian SVM, and weighted

KNN were executed using all features combined and the two groups of features with 46 test points to assess the performance of the proposed feature selection, as shown in Table 3.

Linear SVM and weighted KNN classifiers showed the best performance with 100% accuracy when these 7 features were used (Tables 3 and 4, and Figures 3 and 4). Further, Table 3 illustrates that the average time required for all classifiers to predict one observation when using 7 features is much less compared to the

Table 2: Top-ranked features for the studied algorithms

Features from t-test ranking	t -value	Features from ANOVA ranking	F score	Features from Relief-F ranking	Weight
Right Amygdala	11.8	Cortical thickness_left entorhinal	114.5	Cortical thickness_left entorhinal	0.176
Cortical thickness_left entorhinal	11.71	Right Amygdala	114.4	Left Amygdala	0.135
Left Amygdala	11.02	Right Amygdala	112.2	Left Hippocampus	0.133
Left Hippocampus	10.7	Left Hippocampus	100.4	Cortical thickness_ right entorhinal	0.130
Left Inferior Middle Temporal Gyri	10.66	Left Inferior Middle Temporal Gyri	92.8	Right Hippocampus	0.129
Right Ambient and Parahippocampus Gyri	10.12	Right Ambient and Parahippocampus Gyri	89.1	Right Amygdala	0.124
Right Hippocampus	10.08	Right Hippocampus	88.04	Left Ambient and Parahippocampus Gyri	0.110
Left Ambient and Parahippocampus Gyri	10.06	Left Ambient and Parahippocampus Gyri	87.9	Left Fusiform Gyrus	0.108
Right Inferior Middle Temporal Gyri	9.83	Right Inferior Middle Temporal Gyri	84.7	Right Ambient and Parahippocampus Gyri	0.092
Left Anterior Medial Temporal Lobe	9.74	Left Anterior Medial Temporal Lobe	83.2	Cortical thickness right temporal pole	0.080
Cortical thickness_right entorhinal	9.55	Cortical thickness_right entorhinal	78.69	Cortical thickness left inferior temporal	0.077
Left Posterior Temporal Lobe	9.2	Right Anterior Medial Temporal Lobe	76.4	Left Inferior Middle Temporal Gyri	0.072

Table 3: Accuracy and prediction time for using the original features, 9 common features, and 7 common features.

	Decision tree (%)	Linear SVM (%)	Gaussian SVM (%)	Weighted KNN (%)	Avg prediction time (milliseconds/ one obs) (msec)
Original features	95.65	95.65	93.48	86.95	3
9 common features	93.48	97.83	97.83	97.83	0.7
7 common features	93.48	100.00	97.83	100.00	0.6 msec

SVM: Support Vector Machine, KNN: K-Nearest Neighbors, obs: Observation

Table 4: Classification performance of applied classifiers

	number of features =7			number of features=9		
	precision	sensitivity	specificity	precision	sensitivity	specificity
Decision Tree	0.95	0.9047	0.96	0.95	0.9047	0.96
Linear SVM	1	1	1	0.9545	1	0.96
Gaussian SVM	0.9545	1	0.96	0.9545	1	0.96
Weighted KNN	1	1	1	0.9545	1	0.96

SVM: Support Vector Machine, KNN: K-Nearest Neighbors

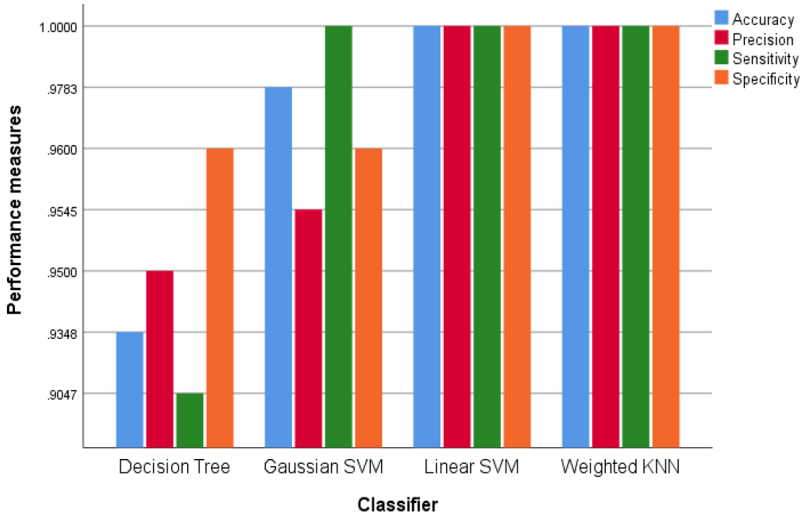

Figure 3: Performance measurements for 7 common features

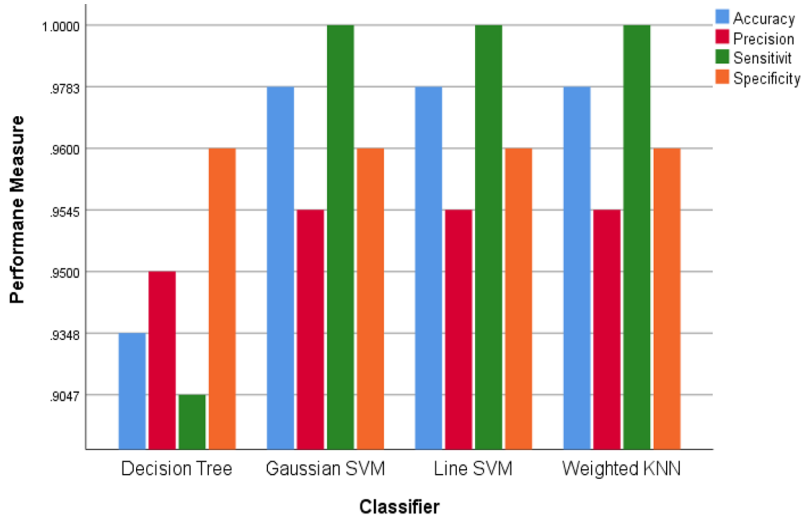

Figure 4: Performance measurements for 9 common features

prediction time for using the original features. As a result, the suggested approach would provide the most critical characteristics with the least time and the greatest accurate outcomes compared to earlier efforts. We considered the following measurements:

$$\text{Sensitivity} = \frac{TP}{(TP+FN)}, \text{Specificity} = \frac{TN}{TN+FP},$$

$$Precision = \frac{TP}{TP+FP}, Accuracy = \frac{TP+TN}{TP+TN+FP+FN}$$

where TP, TN, FP, and FN are true positive, true negative, false positive, and false negative, respectively.

Figure 5 shows that cortical thickness right entorhinal and left inferior middle temporal gyri features, excluded when creating group 2, have large overlapping areas between AD (class 1) and NC (class 2). Therefore, the elimination of them increased the accuracy of detection for LSVM and W- KNN.

Discussion

In this work, 4 machine-learning models were proposed, including decision tree, linear SVM, Gaussian SVM, and weighted KNN for differentiating AD individuals from brain MRI images. Based on the results, linear SVM and weighted KNN achieved the same performance with accuracy of 100% using 7 features. The SVM and KNN provide good performance with 7 and 9 features with sensitivity (recall), selected as the models to decrease missed AD cases as much as possible.

When volume features were combined with surface-based features (CT, SD, and GI), sulcal depth and gyrification index were underestimated. As a result, sulcal depth and gyrification index did not rank amongst the top features. GI and sulcal depth (SD) do not contribute to the detection of AD stage compared to volume features. Therefore, we can rely primarily on the volumes of the hippocampus (left and right), amygdala (left and right), and parahippocampus (left and right) as parts of the limbic brain system. Furthermore, the left cortical thickness of the entorhinal cortex can be added to the previous volume features to improve detection performance.

Table 5 compares various results from previous techniques for detecting Alzheimer's disease and the proposed method. One compared study developed an approach for classifying AD from NC with accuracy up to 92.86% by using fusion of texture and morphemtric features, RFE-SVM for the feature selection process and SVM for the classification process [40]. Another study depended on

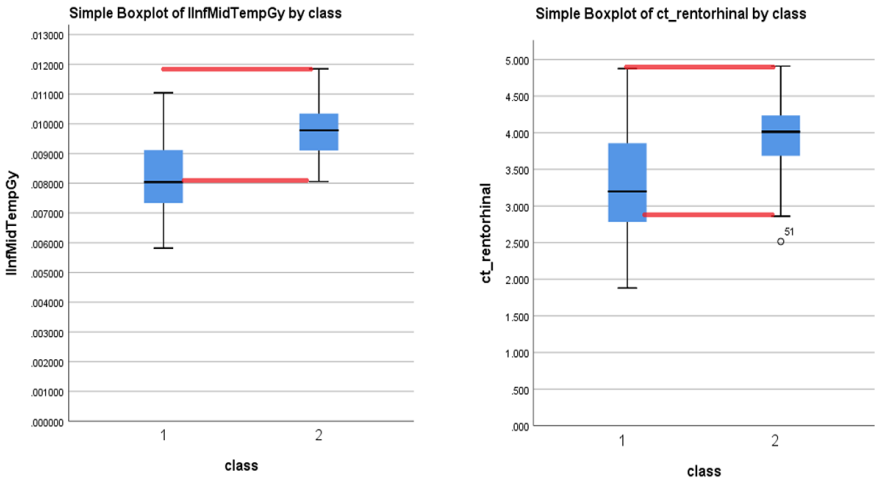

Figure 5: Boxplot of the two excluded features

Table 5: Techniques used in related works

References	Year	AD diagnosis	#Of features	Techniques used	Dataset	Accuracy (%)
[33]	2020	Segmentation And feature extraction, Feature selection, Classification	138 anatomical morphometry: 40 subcortical volumes. 98 cortical thickness.	Segmentation And feature extraction: MALPEM, Feature selection: PCA, Classification: SVM	701 subjects (326 GARD, 123 ADNI, 121 ARWIBO, 131 NACC) AD:168 NC: 274	For GARD data: 95.45
[38]	2011	Feature extraction, feature reduction, classification	20 features	Feature Extraction: VBM, Feature reduction: PCA, Classification: SRAN	OASIS Dataset, Subject=60, AD=30, NC=30	91.18
[39]	2013	Feature extraction, Feature selection, Classification	20 features	Feature extraction: VBM, Feature Selection: PCA, Classification: ELM	OASIS dataset, subjects=218, AD=70, NC=98	94.63 (5788 features) 91 (20 features)
[40]	2015	Feature extraction, Feature selection, Classification	9 features	Feature extraction: Gray-Level Co-occurrence Matrix (GLCM) method and Gabor filter (Texture features) and VBM analysis (Morphometric feature), Feature selection: SVM-RFE, Classification: SVM	ADNI database, subjects=112, AD=54, NC=58	92.86
[41]	2015	Feature extraction, Feature selection, Classification	31 features	Feature extraction: VBM, Feature Selection: RFE, Classification: PBLMcRBFN	OASIS dataset, subjects=60, AD=30, NC=30	89.81
[49]	2020	Data labeling Building, CNN model, Performance evaluation		12 layers CNN	OASIS dataset, subjects= 416, AD=100, NC=316	97.65
[50]	2021	Segmentation, Feature extraction, Classification		Segmentation: 3D deep U-Net, Feature extraction and classification: CNN model	ADNI dataset, AD=194, NC=216	85.9
[51]	2013	Feature extraction, Feature selection, Classification	10 features	Feature extraction: VBM, Feature selection and classification: ICGA with an ELM classifier	OASIS dataset, subjects=60, AD=30, NC=30	91.86
Proposed work	2021	Feature extraction, Feature selection, Classification	7 Features	Feature extraction: ROI Feature selection: ANOVA+t test+ ReliefF, Classification: LSVM, W-KNN	ADNI dataset, Subjects=154, AD=78, NC=76	100

AD: Alzheimer's Disease, NC: Normal Control, OASIS: The Outcome and Assessment Information Set, VBM: Voxel Based Morphometry, PCA: Principle Component Analysis, SRAN: Self Adaptive Resource Allocation Network classifier, ICGA: Integer Coded Genetic Algorithm, ELM: Extreme Learning Machine classifier, SVM-RFE: support vector machine - recursive feature elimination, PBLMcRBFN : projection based learning for meta-cognitive radial basis function network, MALPEM: A package involves software and data files to accomplish a brain extraction and segmentation into 138 cortical and subcortical structures, GARD: Gwangju Alzheimer's disease and Related Dementia dataset, ARWIBO: Alzheimer's Disease Repository Without Borders, NACC: National Alzheimer's Coordinating Center, ADNI: Alzheimer's Disease Neuroimaging Initiative, CNN: Convolutional Neural Network, ROI: Region of Interest, ANOVA: Analysis of variance, W-KNN: Weighted K-Nearest Neighbors

31 morphemtric features selected using RFE algorithm to differentiate between AD and NC with accuracy equal to 89.81% [41]. One report developed a method based on 12 layers convolutional neural network (CNN) model for AD diagnosis with an accuracy of 97.65% using MRI images acquired from OASIS database [49].

The main reason for this output is using a small number of very associated features with AD and removing redundant features. The existence of unrelated features reduces the classification ability of the model and the overall accuracy, showing the enhancement in the models' performance when excluding right cortical thickness of entorhinal and left inferior temporal gyrus features from the 9 features. Furthermore, this study didn't depend on one feature selection methods to select features.

The limitation of the proposed study is to use filter feature selection technique without consideration of the features correlation or dependency.

The presented work can be improved by using the MCI stage in the future, requiring more relevant features and implementation of more feature engineering steps, which we are working on to develop an approach to classify the three stages of Alzheimer's NC, MCI, and AD.

Conclusion

In this study, an efficient classification system for Alzheimer's disease diagnosis is proposed, based on combining more than one feature selection method (t test, one way ANOVA, and Relief-F algorithm) to acquire the most significant features representing AD from a huge pool of features. Furthermore, four classifiers (decision tree, linear SVM, Gaussian SVM, weighted KNN) was applied to select the highest accuracy. The experiment explained that linear SVM and weighted KNN and the following features are the most precise classifiers: left hippocampus, right hippocampus, left amygdala, right amygdala, left ambient and parahippocampus, right ambient and parahippocampus, and cortical thickness_left entorhinal. In addition, combining volume features with cortical thickness features will provide more accurate results than using either volume or cortical thickness independently. However, the traditional techniques of classifiers have been used and applied on extracted features, the maximum accuracy together with the minimum number of features have been collected.

In the future of this study, we plan to implement an approach to classify the three stages of Alzheimer's NC, MCI, AD and to increase the dataset for a robust classification system.

Acknowledgment

Data used in the preparation of this article was acquired from the Alzheimer's Disease Neuroimaging Initiative (ADNI) database (adni.loni.usc.edu). As such, the investigators within the ADNI contributed to the design and implementation of ADNI and/or provided data but did not participate in the analysis or writing of this paper. Data collection and sharing for this project were funded by the Alzheimer's Disease Neuroimaging Initiative (ADNI) (National Institutes of Health Grant U01 AG024904) and DOD ADNI (Department of Defense award number W81XWH-12-2-0012). ADNI is funded by the National Institute on Aging, the National Institute of Biomedical Imaging and Bioengineering, and through generous contributions from the following: AbbVie, Alzheimer's Association; Alzheimer's Drug Discovery Foundation; Araclon Biotech; BioClinica, Inc.; Biogen; Bristol-Myers Squibb Company; CereSpir, Inc.; Cogstate; Eisai Inc.; Elan Pharmaceuticals, Inc.; Eli Lilly and Company; EuroImmun; F. Hoffmann-La Roche Ltd and its affiliated company Genentech, Inc.; Fujirebio; GE Healthcare; IXICO Ltd.;Janssen Alzheimer Immunotherapy Research & Development, LLC.; Johnson & Johnson Pharmaceutical Research & Development LLC.; Lumosity; Lundbeck; Merck & Co., Inc.;Meso Scale Diagnostics, LLC.; NeuroRx Research; Neurotrack Technologies; Novartis Pharmaceuticals Corporation; Pfizer Inc.; Piramal Imaging; Servier; Takeda Pharmaceutical Company; and Transition Therapeutics. The Canadian Institutes of Health Research is providing funds to support

ADNI clinical sites in Canada. Private sector contributions are facilitated by the Foundation for the National Institutes of Health (www.fnih.org). The grantee organization is the Northern California Institute for Research and Education, and the study is coordinated by the Alzheimer's Therapeutic Research Institute at the University of Southern California. ADNI data are disseminated by the Laboratory for Neuro Imaging at the University of Southern California.

Authors' Contribution

EM. Arabi and KS. Ahmed conceived the design of the study. EM. Arabi accomplished the gathering and analyzing of the data, developed and applied the approach of the study, prepared the original draft. KS. Ahmed carried out the critical revision of the manuscript. All the steps of the study were supervised by KS. Ahmed and AS. Mohra All authors have read and agreed to the published version of the manuscript.

Ethical Approval

All data have been taken under the ADNI approval. ADNI protocol and ethics statement: http://adni.loni.usc.edu/wp-content/themes/freshnews-dev-v2/documents/clinical/ADNI-2_Protocol.pdf.

Conflict of Interest

None

References

1. Brookmeyer R, Gray S, Kawas C. Projections of Alzheimer's disease in the United States and the public health impact of delaying disease onset. *Am J Public Health*. 1998;**88**(9):1337-42. doi: 10.2105/ajph.88.9.1337. PubMed PMID: 9736873. PubMed PMCID: PMC1509089.
2. Alzheimer's Association. Why-Get-Checked. 2022 [cited 2022 March 15]. Available from: https://www.alz.org/alzheimers-dementia/diagnosis/why-get-checked.
3. Social Care Institute for Excellence. Dementia: Why early diagnosis of dementia is important. 2022 [cited 2022 March 15]. Available from: https://www.scie.org.uk/dementia/symptoms/diagnosis/early-diagnosis.asp.
4. Arevalo-Rodriguez I, Smailagic N, Roqué I Figuls M, Ciapponi A, Sanchez-Perez E, et al. Mini-Mental State Examination (MMSE) for the detection of Alzheimer's disease and other dementias in people with mild cognitive impairment (MCI). *Cochrane Database Syst Rev.* 2015;**2015**(3):CD010783. doi: 10.1002/14651858.CD010783.pub2. PubMed PMID: 25740785. PubMed PMCID: PMC6464748.
5. Wen J, Thibeau-Sutre E, Diaz-Melo M, Samper-González J, Routier A, et al. Convolutional neural networks for classification of Alzheimer's disease: Overview and reproducible evaluation. *Med Image Anal*. 2020;**63**:101694. doi: 10.1016/j.media.2020.101694. PubMed PMID: 32417716.
6. Bartos A, Gregus D, Ibrahim I, Tintěra J. Brain volumes and their ratios in Alzheimer´s disease on magnetic resonance imaging segmented using Freesurfer 6.0. *Psychiatry Res Neuroimaging*. 2019;**287**:70-74. doi: 10.1016/j.pscychresns.2019.01.014. PubMed PMID: 31003044.
7. Cuingnet R, Gerardin E, Tessieras J, Auzias G, Lehéricy S, et al. Automatic classification of patients with Alzheimer's disease from structural MRI: a comparison of ten methods using the ADNI database. *Neuroimage*. 2011;**56**(2):766-81. doi: 10.1016/j.neuroimage.2010.06.013. PubMed PMID: 20542124.
8. Davatzikos C, Bhatt P, Shaw LM, Batmanghelich KN, Trojanowski JQ. Prediction of MCI to AD conversion, via MRI, CSF biomarkers, and pattern classification. *Neurobiol Aging.* 2011;**32**(12):2322.e19-27. doi: 10.1016/j.neurobiolaging.2010.05.023. PubMed PMID: 20594615. PubMed PMCID: PMC2951483.
9. Braak H, Braak E. Frequency of stages of Alzheimer-related lesions in different age categories. *Neurobiol Aging*. 1997;**18**(4):351-357. doi: 10.1016/s0197-4580(97)00056-0. PubMed PMID: 9330961.
10. Schilling LP, Zimmer ER, Shin M, Leuzy A, Pascoal TA, et al. Imaging Alzheimer's disease pathophysiology with PET. *Dement Neuropsychol.* 2016;**10**(2):79-90. doi: 10.1590/S1980-5764-2016DN1002003. PubMed PMID: 29213438. PubMed PMCID: PMC5642398.
11. Marcus C, Mena E, Subramaniam RM. Brain PET in the diagnosis of Alzheimer's disease. *Clin Nucl Med.* 2014;**39**(10):e413-26. doi: 10.1097/RLU.0000000000000547. PubMed PMID: 25199063. PubMed PMCID: PMC4332800.
12. Gray KR, Wolz R, Heckemann RA, Aljabar P, et al. Multi-region analysis of longitudinal FDG-PET for the classification of Alzheimer's disease. *Neuroimage*. 2012;**60**(1):221-9. doi: 10.1016/j.neuroimage.2011.12.071. PubMed PMID: 22236449. PubMed PMCID: PMC3303084.

13. Nordberg A, Rinne JO, Kadir A, Långström B. The use of PET in Alzheimer disease. *Nat Rev Neurol.* 2010;**6**(2):78-87. doi: 10.1038/nrneurol.2009.217. PubMed PMID: 20139997.
14. Ou YN, Xu W, Li JQ, Guo Y, Cui M, Chen KL, et al. FDG-PET as an independent biomarker for Alzheimer's biological diagnosis: a longitudinal study. *Alzheimers Res Ther*. 2019;**11**(1):57. doi: 10.1186/s13195-019-0512-1. PubMed PMID: 31253185. PubMed PMCID: PMC6599313.
15. Graña M, Termenon M, Savio A, Gonzalez-Pinto A, Echeveste J, Pérez JM, Besga A. Computer aided diagnosis system for Alzheimer disease using brain diffusion tensor imaging features selected by Pearson's correlation. *Neurosci Lett.* 2011;**502**(3):225-9. doi: 10.1016/j.neulet.2011.07.049. PubMed PMID: 21839143.
16. Lee W, Park B, Han K. Classification of diffusion tensor images for the early detection of Alzheimer's disease. *Comput Biol Med*. 2013;**43**(10):1313-20. doi: 10.1016/j.compbiomed.2013.07.004. PubMed PMID: 24034721.
17. Sørensen L, Igel C, Pai A, Balas I, Anker C, et al. Differential diagnosis of mild cognitive impairment and Alzheimer's disease using structural MRI cortical thickness, hippocampal shape, hippocampal texture, and volumetry. *Neuroimage Clin*. 2016;**13**:470-82. doi: 10.1016/j.nicl.2016.11.025. PubMed PMID: 28119818. PubMed PMCID: PMC5237821.
18. Achterberg HC, Van Der Lijn F, Den Heijer T, Vernooij MW, Ikram MA, et al. Hippocampal shape is predictive for the development of dementia in a normal, elderly population. *Hum Brain Mapp*. 2014;**35**(5):2359-71. doi: 10.1002/hbm.22333. PubMed PMID: 24039001. PubMed PMCID: PMC6869385.
19. Madusanka N, Choi HK, So JH, Choi BK. Alzheimer's Disease Classification Based on Multi-feature Fusion. *Curr Med Imaging Rev*. 2019;**15**(2):161-9. doi: 10.2174/1573405614666181012102626. PubMed PMID: 31975662.
20. Sørensen L, Igel C, Liv Hansen N, Osler M, Lauritzen M, et al. Early detection of Alzheimer's disease using MRI hippocampal texture. *Hum Brain Mapp*. 2016;**37**(3):1148-61. doi: 10.1002/hbm.23091. PubMed PMID: 26686837. PubMed PMCID: PMC6867374.
21. Liu T, Lipnicki DM, Zhu W, Tao D, Zhang C, Cui Y, Jin JS, Sachdev PS, Wen W. Cortical gyrification and sulcal spans in early stage Alzheimer's disease. *PLoS One*. 2012;**7**(2):e31083. doi: 10.1371/journal.pone.0031083. PubMed PMID: 22363554. PubMed PMCID: PMC3283590.
22. Racine AM, Brickhouse M, Wolk DA, et al. The personalized Alzheimer's disease cortical thickness index predicts likely pathology and clinical progression in mild cognitive impairment. *Alzheimers Dement (Amst)*. 2018;**10**:301-10. doi: 10.1016/j.dadm.2018.02.007. PubMed PMID: 29780874. PubMed PMCID: PMC5956936.
23. Cai K, Xu H, Guan H, Zhu W, Jiang J, Cui Y, Zhang J, Liu T, Wen W. Identification of Early-Stage Alzheimer's Disease Using Sulcal Morphology and Other Common Neuroimaging Indices. *PLoS One*. 2017;**12**(1):e0170875. doi: 10.1371/journal.pone.0170875. PubMed PMID: 28129351. PubMed PMCID: PMC5271367.
24. Boutet C, Chupin M, Lehéricy S, Marrakchi-Kacem L, Epelbaum S, et al. Detection of volume loss in hippocampal layers in Alzheimer's disease using 7 T MRI: a feasibility study. *Neuroimage Clin.* 2014;**5**:341-8. doi: 10.1016/j.nicl.2014.07.011. PubMed PMID: 25161900. PubMed PMCID: PMC4141975.
25. Braak H, Braak E. Neuropathological stageing of Alzheimer-related changes. *Acta Neuropathol*. 1991;**82**(4):239-59. doi: 10.1007/BF00308809. PubMed PMID: 1759558.
26. Poulin SP, Dautoff R, Morris JC, et al. Amygdala atrophy is prominent in early Alzheimer's disease and relates to symptom severity. *Psychiatry Res*. 2011;**194**(1):7-13. doi: 10.1016/j.pscychresns.2011.06.014. PubMed PMID: 21920712. PubMed PMCID: PMC3185127.
27. Prestia A, Boccardi M, Galluzzi S, Cavedo E, Adorni A, et al. Hippocampal and amygdalar volume changes in elderly patients with Alzheimer's disease and schizophrenia. *Psychiatry Res*. 2011;**192**(2):77-83. doi: 10.1016/j.pscychresns.2010.12.015. PubMed PMID: 21458960.
28. Weiner MW, Veitch DP, Aisen PS, Beckett LA, Cairns NJ, et al. The Alzheimer's Disease Neuroimaging Initiative: a review of papers published since its inception. *Alzheimers Dement.* 2012;**8**(1 Suppl):S1-68. doi: 10.1016/j.jalz.2011.09.172. PubMed PMID: 22047634. PubMed PMCID: PMC3329969.
29. Devanand DP, Bansal R, Liu J, Hao X, Pradhaban G, Peterson BS. MRI hippocampal and entorhinal cortex mapping in predicting conversion to Alzheimer's disease. *Neuroimage.* 2012;**60**(3):1622-9. doi: 10.1016/j.neuroimage.2012.01.075. PubMed PMID: 22289801. PubMed PMCID: PMC3320768.
30. Rohini P, Sundar S, Ramakrishnan S. Charac-

terization of Alzheimer conditions in MR images using volumetric and sagittal brainstem texture features. *Comput Methods Programs Biomed*. 2019;**173**:147-55. doi: 10.1016/j.cmpb.2019.03.003. PubMed PMID: 31046989.

31. Apostolova LG, Green AE, Babakchanian S, Hwang KS, Chou YY, Toga AW, Thompson PM. Hippocampal atrophy and ventricular enlargement in normal aging, mild cognitive impairment (MCI), and Alzheimer Disease. *Alzheimer Dis Assoc Disord*. 2012;**26**(1):17-27. doi: 10.1097/WAD.0b013e3182163b62. PubMed PMID: 22343374. PubMed PMCID: PMC3286134.
32. Klöppel S, Stonnington CM, Chu C, Draganski B, Scahill RI, et al. Automatic classification of MR scans in Alzheimer's disease. *Brain*. 2008;**131**(Pt 3):681-9. doi: 10.1093/brain/awm319. PubMed PMID: 18202106. PubMed PMCID: PMC2579744.
33. Toshkhujaev S, Lee KH, Choi KY, Lee JJ, Kwon GR, Gupta Y, Lama RK. Classification of Alzheimer's Disease and Mild Cognitive Impairment Based on Cortical and Subcortical Features from MRI T1 Brain Images Utilizing Four Different Types of Datasets. *J Healthc Eng*. 2020;**2020**:3743171. doi: 10.1155/2020/3743171. PubMed PMID: 32952988. PubMed PMCID: PMC7482016.
34. Zhu Y, Huang C. An improved median filtering algorithm for image noise reduction. *Physics Procedia*. 2012;**25**:609-16. doi: 10.1016/j.phpro.2012.03.133.
35. Kruthika KR, Rajeswari H, Maheshappa HD. Multistage classifier-based approach for Alzheimer's disease prediction and retrieval. *Informatics in Medicine Unblocked*. 2019;**14**:34-42. doi:10.1016/j.imu.2018.12.003.
36. Acharya UR, Fernandes SL, WeiKoh JE, Ciaccio EJ, et al. Automated Detection of Alzheimer's Disease Using Brain MRI Images- A Study with Various Feature Extraction Techniques. *J Med Syst*. 2019;**43**(9):302. doi: 10.1007/s10916-019-1428-9. PubMed PMID: 31396722.
37. Beheshti I, Demirel H, Matsuda H. Classification of Alzheimer's disease and prediction of mild cognitive impairment-to-Alzheimer's conversion from structural magnetic resource imaging using feature ranking and a genetic algorithm. *Comput Biol Med*. 2017;**83**:109-19. doi: 10.1016/j.compbiomed.2017.02.011. PubMed PMID: 28260614.
38. Mahanand BS, Suresh S, Sundararajan N, Kumar M. Alzheimer's disease detection using a Self-adaptive Resource Allocation Network classifier. The 2011 International Joint Conference on Neural Networks; San Jose, CA, USA: IEEE; 2011.
39. Kumar MA, Mahanand BS. Alzheimer's Disease Detection Using Minimal Morphometric Features with an Extreme Learning Machine Classifier. International Conference on Advances in Computing; New Delhi: Springer; 2013. doi: 10.1007/978-81-322-0740-5_90.
40. Ding Y, Zhang C, Lan T, Qin Z, Zhang X, Wang W. Classification of Alzheimer's disease based on the combination of morphometric feature and texture feature. 2015 IEEE International Conference on Bioinformatics and Biomedicine (BIBM); Washington, DC, USA: IEEE; 2015. p. 409-12. doi: 10.1109/BIBM.2015.7359716.
41. Mahanand BS, Babu GS, Suresh S, Sundararajan N. Identification of Imaging Biomarkers Responsible for Alzheimer's Disease using a McRBFN Classifier. 2015 International Conference on Cognitive Computing and Information Processing (CCIP); Noida, India: IEEE; 2015. doi: 10.1109/CCIP.2015.7100723.
42. Hammers A, Allom R, Koepp MJ, Free SL, Myers R, Lemieux L, Mitchell TN, Brooks DJ, Duncan JS. Three-dimensional maximum probability atlas of the human brain, with particular reference to the temporal lobe. *Hum Brain Mapp*. 2003;**19**(4):224-47. doi: 10.1002/hbm.10123. PubMed PMID: 12874777. PubMed PMCID: PMC6871794.
43. Kira K, Rendell LA. The feature selection problem: Traditional methods and a new algorithm. AAAI-92: Proceedings of the 10th National Conference on Artificial Intelligence; San Jose, California: AAAI Press; 1992. p. 129-34.
44. Kononenko I, Bergadano F, Luc D. Estimating attributes: analysis and extensions of relief. European Conference on Machine Learning; Berlin, Heidelberg: Springer; 1994. p. 171-82. doi: 10.1007/3-540-57868-4_57.
45. Zhou X, Wang J. Feature Selection for Image Classification Based on a New Ranking Criterion. *Journal of Computer and Communications*. 2015;3(3):74-9. doi: 10.4236/jcc.2015.33013.
46. Liu M, Zhang D, Shen D. Ensemble sparse classification of Alzheimer's disease. *Neuroimage*. 2012;**60**(2):1106-16. doi: 10.1016/j.neuroimage.2012.01.055. PubMed PMID: 22270352. PubMed PMCID: PMC3303950.
47. Chaves R, Ramírez J, Górriz JM, López M, Salas-Gonzalez D, Alvarez I, Segovia F. SVM-based computer-aided diagnosis of the Alzheimer's disease using t-test NMSE feature selection with feature correlation weighting. *Neurosci Lett*. 2009;**461**(3):293-7. doi: 10.1016/j.neulet.2009.06.052. PubMed PMID: 19549559.

48. Keerthi SS, Lin CJ. Asymptotic behaviors of support vector machines with Gaussian kernel. *Neural Comput.* 2003;**15**(7):1667-89. doi: 10.1162/089976603321891855. PubMed PMID: 12816571.
49. Hussain E, Hasan M, Hassan SZ, Azmi TH, Rahman MA, Parvez MZ. Deep Learning Based Binary Classification for Alzheimer's Disease Detection using Brain MRI Images. 15th IEEE Conference on Industrial Electronics and Applications (ICIEA); Kristiansand, Norway: IEEE Xplore; 2020. p. 1115-20. doi: 10.1109/ICIEA48937.2020.9248213.
50. Li A, Li F, Elahifasaee F, Liu M, Zhang L. Hippocampal shape and asymmetry analysis by cascaded convolutional neural networks for Alzheimer's disease diagnosis. *Brain Imaging Behav.* 2021;**15**(5):2330-9. doi: 10.1007/s11682-020-00427-y. PubMed PMID: 33398778.
51. Mahanand BS, Suresh S, Sundararajan N, Kumar M. ICGA-ELM classifier for Alzheimer's disease detection. 2013 Indian Conference on Medical Informatics and Telemedicine (ICMIT); Kharagpur, India: IEEE; 2013. p. 48-52. doi: 10.1109/IndianCMIT.2013.6529407.